TECHNIQUE FOR MEASURING THE DIELECTRIC CONSTANT OF THIN MATERIALS

K. Sarabandi and F. T. Ulaby
The University of Michigan

ABSTRACT

A practical technique for measuring the dielectric constant of vegetation leaves and similarly thin materials is presented. A rectangular section of the leaf is placed in the transverse plane in a rectangular waveguide and the magnitude and phase of the reflection coefficient are measured over the desired frequency band using a vector network analyzer. By treating the leaf as an infinitesimally thin resistive sheet, an explicit expression for its dielectric constant is obtained in terms of the reflection coefficient. Because of the thin-sheet approximation, however, this approach is valid only at frequencies below 1.5 GHz. To extend the technique to higher frequencies, higher order approximations are derived and their accuracies are compared to the exact dielectric-slab solution. For a material whose thickness is 0.5 mm or less, the proposed technique was found to provide accurate values of its dielectric constant up to frequencies of 12 GHz or higher. The technique was used to measure the 8-12 GHz dielectric spectrum for vegetation leaves, teflon, and rock samples.

This work was supported by the National Aeronautics and Space Administration under Contract NAG5-480.

I. INTRODUCTION

Prompted by the need for a practical technique for measuring the microwave dielectric constant of vegetation leaves, solutions were sought for the voltage reflection coefficient measured at the input of a rectangular waveguide containing a thin slab placed in a plane orthogonal to the propagation direction (Fig. 1). The slab is modeled in Section II as a resistive-current-sheet [1,2], which has proved to be an excellent approach for characterizing the radar-cross-section of a vegetation leaf over a wide range of moisture conditions (and a correspondingly wide range of the relative dielectric contstant ε).

To evaluate the accuracy of the technique for measuring the real and imaginary parts of ε from measurements of the complex reflection coefficient Γ, an exact solution for Γ of the slab will be obtained in Section III and then used to simulate the measurement process for given values of ε. The evaluation is performed in Section IV by comparing the true value of ε with that predicted by the resistive-current-sheet expression. It turns out that the resistive-current-sheet solution is identical with the zeroth-order approximation of the exact solution for Γ. One of the attractive features of the zeroth-order solution is that it provides an explicit expression for ε in terms of Γ.

The evaluation shows that the zeroth-order solution provides an excellent estimate for the real part of the dielectric constant, ε', if the slab thickness τ is sufficiently small to satisfy the condition $\tau \leq 0.05\,\lambda_0\sqrt{|\varepsilon|}$, where λ_0 is the free-space wavelength. For a typical leaf-thickness of 0.3 mm, this condition is satisfied for any moisture

condition if the frequency $f \leq 15$ GHz. A much more stringent condition on τ is required in order for the zeroth-order solution to give accurate values for ε''; namely $\tau \leq 0.01\,\lambda_0\sqrt{|\varepsilon|}$ and $\varepsilon''/\varepsilon' \geq 0.1$, or equivalently, $f \leq 1.5$ GHz for vegetation leaves.

To relax this limitation, alternate solutions for Γ are obtained in Section III by invoking approximations that lead to first-order and second-order solutions whose forms are invertible to explicit expressions for ε. Use of the second-order solution is found to extend the frequency range from 1.5 GHz to 12 GHz for a leaf with a high moisture content and to higher frequencies for drier leaves.

Section V presents 8-12 GHz spectra of the dielectric constant ε for vegetation leaves, teflon and rock slices, all measured using the technique developed in this paper. Where possible, the results are compared with measurements made by other techniques.

II. MODEL FOR A THIN RESISTIVE SHEET

Consider the rectangular waveguide diagrammed in Fig. 1(a). The guide is terminated with a matched load, has dimensions a x b, and contains a thin resistive sheet of thickness τ at $z = 0$. The waveguide dimensions are such that only the TE_{10} mode can propagate in the guide.

We seek a relationship between the input voltage reflection coefficient Γ and the relative complex dielectric constant of the sheet material ε. To this end, we shall develop expressions for the electric and magnetic fields in Regions I and II and then

apply the appropriate boundary conditions. If ψ_I and ψ_{II} are the electric potentials in regions I and II, respectively, solutions of the scalar Helmholtz equation

$$\left(\nabla^2 + k^2\right) \Psi_{I,II} = 0 \ , \tag{1}$$

for the TE_{10} mode leads to [4, pp. 148-149]:

$$\psi_I = \cos\left(\frac{\pi x}{a}\right)\left[C_1 \, e^{i k_z z} + C_2 \, e^{-i k_z z} \right] \ ; z \geq 0 \tag{2}$$

$$\psi_{II} = \cos\left(\frac{\pi x}{a}\right) \cdot C_3 \, e^{i k_z z} \qquad ; z \leq 0 \ , \tag{3}$$

where a time factor $e^{i\omega t}$ was asssumed and suppressed. The constants C_1 and C_2 represent the magnitudes of the incident and reflected waves in Region I, C_3 represents the magnitude of the wave traveling towards the matched load in Region II, and

$$k_z = \sqrt{k^2 - \left(\frac{\pi}{a}\right)^2} = \frac{\pi}{\lambda a}\sqrt{4a^2 - \lambda^2} \ . \tag{4}$$

The components of $\bar{E}$ and $\bar{H}$ may be obtained from (2) and (3) by applying the relations [4, p. 130].

$$\bar{E} = -\nabla \times (\psi \hat{z}) \ , \qquad \bar{H} = -i\omega\varepsilon(\psi \hat{z}) + \frac{1}{i\omega\mu} \nabla\nabla \cdot (\psi \hat{z}) \ . \tag{5}$$

The resistive sheet model [1] treats the sheet in the plane $z = 0$ as infinitesimally thin carrying an induced tangential electric current $\bar{J}$ that is related to $\bar{E}$ by

$$\hat{n} \times \hat{n} \times \bar{E} = -R\bar{J} , \tag{6}$$

where $\hat{n}$ is the surface normal of the sheet ($\hat{n} = \hat{z}$ in Region I and $\hat{n} = -\hat{z}$ in Region II) and R is the sheet resistivity,

$$R = \frac{-i\,\eta_0}{k\,\tau(\varepsilon - 1)} , \qquad \text{ohms per square meter.} \tag{7}$$

In the above expression, $k = 2\pi / \lambda_0$, τ is the sheet thickness, η_0 is the free space intrinsic impedance, and

$$\varepsilon = \varepsilon' - i\,\varepsilon'', \tag{8}$$

is its relative complex dielectric constant. The condition for continuity of the tangential electric field from Region I to Region II and the boundary condition for the magnetic field requires that

$$\hat{z} \times \left(\bar{E}_I - \bar{E}_{II}\right) = 0 , \qquad \hat{z} \times \left(\bar{H}_I - \bar{H}_{II}\right) = \bar{J} , \tag{9}$$

The unknown coefficients C_1, C_2, C_3 can be obtained by applying the boundary conditions given by (6) and (9). The complex voltage reflection coefficient is then found to be

$$\Gamma = \frac{C_2}{C_1} = -\frac{k^2\,\tau(\varepsilon - 1)}{k^2\,\tau(\varepsilon - 1) - 2i\,k_z} , \tag{10}$$

from which an explicit expression for ε is obtained,

$$\varepsilon = 1 + \frac{2 i k_z \Gamma}{k^2 \tau (1 + \Gamma)} = 1 + \frac{i\left(\frac{\lambda}{2\pi a}\right)\sqrt{4a^2 - \lambda^2}}{\tau (1 + 1/\Gamma)} . \qquad (11)$$

Thus, by measuring the complex reflection coefficient Γ and the sheet thickness τ we can compute ε directly. This technique can be very useful for measuring the dielectric constant of vegetation leaves and other similarly thin slabs. Its success, however, depends on two factors: (a) the ability to measure both the magnitude and phase of Γ accurately, which now is possible with the HP-8510 vector network analyzer, and (b) the validity of the thin-sheet assumption underlying the derivation that led to (11). To examine the range of validity of this assumption and to quantify it in the form of specific limits, we shall first derive the expression for the reflection coefficient when a dielectric slab of arbitrary thickness is placed in the waveguide, and then compare the exact solution with the solution given by (10) and (11).

III. MODEL FOR A SLAB OF ARBITRARY THICKNESS

The waveguide section shown in Fig. 2 is terminated in a matched load and contains a dielectric slab extending from $z = 0$ to $z = -\tau$. The electric potentials in regions I, II, and III are

$$\Psi_I = \cos\left(\frac{\pi x}{a}\right)\left[C_1 e^{i k_z z} + C_2 e^{-i k_z z}\right] \quad ; \quad z \geq 0 \qquad (12)$$

$$\Psi_{II} = \cos\left(\frac{\pi x}{a}\right)\left[C_3 e^{i k_{z2} z} + C_4 e^{-i k_{z2} z}\right] \quad ; \quad 0 \geq z \geq -\tau \qquad (13)$$

$$\Psi_{III} = \cos\left(\frac{\pi x}{a}\right) \cdot C_5 e^{i k_z z} \qquad -\tau \geq z \qquad (14)$$

where k_z is given by (4) and k_{z2} is given by

$$k_{z2} = \frac{\pi}{\lambda a} \sqrt{4 \varepsilon a^2 - \lambda^2} \quad . \qquad (15)$$

Upon using the relations given by (5) to obtain $\bar{E}$ and $\bar{H}$ in each of the three regions, and then applying the continuity conditions of the tangential $\bar{E}$ and $\bar{H}$ fields at the boundaries $z = 0$ and $z = -\tau$, we obtain the following expression for the reflection coefficient

$$\Gamma = \frac{C_2}{C_1} = \frac{-i\left[\left(k_{z2}/k_z\right)^2 - 1\right] \sin\left(k_{z2}\tau\right)}{2\left(\frac{k_{z2}}{k_z}\right) \cos\left(k_{z2}\tau\right) + i\left[\left(k_{z2}/k_z\right)^2 + 1\right] \sin\left(k_{z2}\tau\right)} \quad . \qquad (16)$$

We shall refer to (16) as the exact solution for Γ.

Second-Order Solution

If $k_{z2}\tau$ is small and we use the approximations

$$\sin k_{z2}\tau \equiv k_{z2}\tau \qquad (17a)$$

$$\cos k_{z2}\tau \cong 1 - \frac{1}{2}\left(k_{z2}\tau\right)^2 \quad , \qquad (17b)$$

The expressions given by (16) can be simplified to give the *second-order* solution

$$\Gamma \cong \frac{-(\varepsilon-1)}{\left(1-\frac{1}{2}\left(\frac{\lambda}{a}\right)^2 - i\tau k_z\left(\frac{\lambda}{2a}\right)^2 - 2ik_z/\tau k^2\right) + \left(1+i\tau k_z\right)\varepsilon}, \tag{18}$$

from which we obtain the following explicit expression for the *second-order* solution of the relative dielectric constant,

$$\varepsilon \stackrel{\Delta}{=} \varepsilon_2 \cong \frac{1-\left[1-\frac{1}{2}\left(\frac{\lambda}{a}\right)^2 - i\tau k_z\left(\frac{\lambda}{2a}\right)^2 - 2ik_z/\tau k^2\right]\Gamma}{1+\left(1+i\tau k_z\right)\Gamma}. \tag{19}$$

First-Order Solution

If, instead of the approximation given by (17b), we were to set $\cos k_{2z}\tau \cong 1$ in (16) (i.e., ignoring second and higher order powers of $(k_{z2}\tau)$), we would obtain the result

$$\Gamma \cong \frac{-1}{\left[\varepsilon+\left(1-\frac{1}{2}\left(\frac{\lambda}{a}\right)^2\right)\right]/(\varepsilon-1) - 2ik_z/\left(\tau k^2(\varepsilon-1)\right)}, \tag{20}$$

which can then be solved to obtain the expression

$$\varepsilon \stackrel{\Delta}{=} \varepsilon_1 \cong \frac{1-\left[1-\left(\lambda^2/2a^2\right)-2ik_z/\tau k^2\right]\Gamma}{(1+\Gamma)}, \tag{21}$$

for the first-order estimate of ε.

Zeroth-Order Solution

If $\varepsilon >> 1$, we may use the approximation

$$\frac{\varepsilon + \left(1 - \frac{1}{2}\left(\frac{\lambda}{a}\right)^2\right)}{\varepsilon - 1} \cong 1 \tag{21}$$

because $-1 \le 1 - \frac{1}{2}(\lambda/a)^2 < 1$. Equation (20) then leads to

$$\varepsilon \stackrel{\Delta}{=} \varepsilon_0 \cong 1 + \frac{2 i k_z \Gamma}{\tau k^2 (\Gamma + 1)} = 1 + \frac{i (\lambda / 2 \pi a) \sqrt{4 a^2 - \lambda^2}}{\tau (1 + 1/\Gamma)} . \tag{22}$$

which is identical with the resistive-sheet approximation given by (11).

IV. SENSITIVITY ANALYSIS

The second order solution for Γ, given by (18), was based on assuming that $k_{z2}\,\tau << 1$ and on retaining terms up to and including power of 2 in the series expressions for $\sin k_{z2}\,\tau$ and $\cos k_{z2}\,\tau$, as indicated by (17). In the first-order solution, only the zeroth- and first-order terms were retained. The purpose of these derivations is to use them for computing ε from measured values of the complex reflection coefficient Γ. The accuracies of the approximate expressions given by (19) and (21), corresponding to the second-order and first-order solutions for ε, respectively, depends on the magnitude of $k_{z2}\,\tau$. For a standard waveguide operated

in the TE_{10} mode, the dimension a is on the order of $3\lambda/4$. Hence,

$$k_{z2}\tau = k\tau\sqrt{\varepsilon - (\lambda/2a)^2} \cong k\tau\sqrt{\varepsilon - 4/9} \ .$$

If we require that $k\tau\sqrt{\varepsilon}$ be small, then k_{z2} will be smaller still.

The zeroth-order solution (22) is only applicable if ε is sufficiently large to allow the approximation given by (21) to be used in (20). Hence for ε large, the first-order and zeroth-order solutions should yield comparable results.

To evaluate these approximate expressions for ε, we conducted the following sensitivity analysis. We selected specific values of the waveguide width a, the wavelength λ, and the relative complex dielectric constant of the slab, ε. We then computed Γ using the exact solution (16). The computed value of Γ was then used in (22), (21), and (19) to compute the zeroth-order, first-order, and second-order estimates of ε. We denote these ε_0, ε_1, and ε_2.

Our first example of this procedure is Fig. 3 where we show plots of ε_0, ε_1, and ε_2 at 10 GHz as a function of τ for a slab with true dielectric constant $\varepsilon = 2 - i\,0.01$. We observe that ε_0', ε_1', and ε_2' in Fig. 3(a) each provide values that are within 1 percent of ε' for $\tau \leq 1$ mm. Amongst the three approximations, ε_0' is the most accurate, in spite of the fact that the left-hand side of (21) is equal to 2, rather than approximately equal to 1 as required by (21). This insensitivity of Γ to the first term in the denominator of (20) is because this term is much smaller than the second term in

the demoninator of (20), thereby exercising a minor influence on the final expression for ε'.

Measuring ε' of a material usually is not a difficult problem, but measuring ε'' of a low-loss material can be. The errors associated with using the approximations leading to $\varepsilon''_0, \varepsilon''_1, \varepsilon''_2$ are shown in Fig. 3(b) in the form of deviations from the true value $\varepsilon'' = 0.01$. For $\tau \leq 1$ mm, the relative error is 20 percent for ε''_2, 50 percent for ε''_1, and the estimate provided by ε''_0 is grossly inaccurate. Hence, in spite of the result that ε'_0 provides a good estimate of ε', the zeroth-order solution is inadequate for estimating ε''.

Figure 4 shows results for a material with $\varepsilon = 20 - i\,10$. Again ε'_0 provides an adequate estimate of ε' over a wide range of the thickness τ. For the imaginary part, however, ε''_2 consistently provides more accurate estimates of ε'' than those provided by either ε''_0 or ε''_1.

A summary of the relative accuracies of the three approximations $\varepsilon_0, \varepsilon_1$, and ε_2, is presented in Table 1 for slab thicknesses τ equal to 1 percent and 5 percent of $\lambda_0 / \sqrt{|\varepsilon|}$. The entries in the table are the maximum relative errors in percent. For ε'_0, for example, the maximum relative error is defined as

$$e'_0 = \max \left| \frac{\varepsilon'_0 - \varepsilon'}{\varepsilon'} \right| \times 100$$

where ε'_0 is the value provided by (22) and ε' is the true value of the slab permittivity.

V. DIELECTRIC MEASUREMENTS

A. Measurement System

A HP-8510A vector network analyzer was used in conjunction with a HP-8511 parameter test set and a HP-9000 computer (Fig. 5) to measure the amplitude and phase of the reflection coefficient Γ of dielectric slabs placed in a waveguide sample-holder. The arrangement shown in Fig. 5 consists of a waveguide section connected to the HP-8511 through a coax-to-waveguide adapter on one end and to a waveguide section terminated in a matched load on the other end. A thin piece of styrofoam is placed in the sample-holder section at a distance τ from the waveguide opening (junction between the two waveguide sections) where τ is equal to the thickness of the dielectric sample. Another thin piece of styrofoam is placed on the other side of the sample (in the empty waveguide section) to keep the sample in place.

After placing the sample in the waveguide, the network analyzer is used to measure the complex reflection coefficient over the frequency range of interest. In the present setup, the frequency coverage is from 8 GHz to 12 GHz.

B. Measurement Accuracy

The accuracy of the dielectric-constant measurement is critically based upon the accuracy with which the reflection coefficient Γ can be measured. The measurement of Γ may contain some random, nonrepeatable errors caused by system noise and environmental variations as well as certain systematic errors that are repeatable and, therefore, correctable. To correct the systematic errors, the measurement system is calibrated using three independent standards whose reflection coefficients are known

over the frequency range under consideration. These include a short-circuited load, a matched load, and an offset short.

C. Sample Measurements

The technique described in the previous sections was used to measure the 8-12 GHz dielectric spectra of three types of rock materials (each cut in the shape of a thin slab with a cross-section equal to that of the waveguide's) and a thin leaf of vegetation material with a gravimetric moisture content of 90 percent. In addition, a thin slab of teflon with $\varepsilon = 2.0 - j\,0.005$ was measured also. The results are given in Figs. 6 and 7. The results for teflon were found to be in excellent agreement with those measured for a thick sample for both ε' and ε''. The measured permittivities of the rock samples are essentially constant over the 8-12 GHz band (Fig. 6(a)), and for two of the samples (rhyolite and rhyodlacite) the measured permittivity compares very well with values measured by a coaxial probe using an approximate reflection technique [5].

The plots in Fig. 6(b) display ε'', the relative dielectric loss factor, for teflon and the three rock samples. We have no reason to expect ε of rocks to exhibit a dispersive behavior in the 8-12 GHz frequency region, and therefore, we suspect that the observed variability, particularly in the 8-9 GHz range, is an artifact of the measurement system.

The example shown in Fig. 7 is for a leaf of vegetation. Its gravimetric moisture was 0.9 and its thickness 0.23 mm. The continuous curves represent the values of ε' and ε'' measured with the waveguide technique and the circles represent values

calculated using a model [3] with an accuracy of ±20 percent. Within this range of accuracy, the data and the model are in good agreement.

VI. CONCLUSIONS

The technique presented in this paper for measuring the dielectric constant of thin slabs is based on measuring the complex reflection coefficient of the input of a waveguide section with the slab placed in the transverse plane of the waveguide. The dielectric constant of the leaf is then calculated from the measured reflection coefficient.

An explicit expression for the dielectric constant is obtained in terms of the reflection coefficient by simplifying the exact solution for reflection from a dielectric slab using a thin-sheet approximation. The technique is found to provide accurate measurements of the complex dielectric constant for natural materials, including vegetation leaves and rocks, up to 12 GHz if the thickness is 0.55 mm or less.

It is worth mentioning that the technique can be extended to measure the relative permeability by modifying equation (12) to (14). Because such a modification results in having four unknowns, it will be necesary to measure the reflection coefficient corresponding to two different sample thicknesses in order to determine both ε and μ. Alternatively, one can measure the reflection and transmission coefficients of one sample to realize the same objective.

REFERENCES

[1] Harrington, R. F. and J. R. Mautz, "An Impedance Sheet Approximation for Thin Dielectric Shells," *IEEE Trans. Antennas Propagation,* Vol. 23, 1975, pp. 532-534.

[2] Senior, T. B. A., K. Sarabandi, and F. T. Ulaby, "Measuring and Modeling the Backscattering Cross Section of a Leaf," *Radio Science,* Vol. 22, No. 6, November 1987, pp. 1109-1116.

[3] Ulaby, F. T. and M. A. El-Rayes, "Microwave Dielectric Spectrum of Vegetation - Part II: Dual-Dispersion Model," *IEEE Trans. of Geoscience and Remote Sensing.,* Vol. GE-25, No. 5, 1987, pp. 550-557.

[4] Harrington, R. F. (1961), Time-Harmonic Electromagnetic Fields, McGraw-Hill, New York, p. 130.

[5] El-Rayes, M. A. and F. T. Ulaby, "Microwave Dielectric Spectum of Vegetation - Part I: Experimental Observations," *IEEE Trans. of Geoscience and Remote Sensing.,* Vol. GE-25, No. 5, 1987, pp. 541-549.

LIST OF FIGURES

Fig. 1 Rectangular waveguide with thin resistive sheet of thickness τ at $z = 0$.

Fig. 2 Rectangular waveguide with a dielectric slab occupying region II (between $z = 0$ and $z = -\tau$).

Fig. 3 Relative (a) permittivities ε_0', ε_1', and ε_2', and (b) dielectric loss factors.

Fig. 4 Relative (a) permittivities ε_0', ε_1', and ε_2', and (b) dielectric loss factors.

Fig. 5 Measurement system.

Fig. 6 Measured (a) relative permittivity and (b) dielectric loss factor of teflon and three rock samples.

Fig. 7 Measured relative dielectric constant of a vegetation leaf.

LIST OF TABLE

Table 1. Maximum relative errors associated with the expressions for ε_0, ε_1, and ε_2; the quantity e'_0 is defined as: $e'_0 = \max \left| \frac{\varepsilon' - \varepsilon'_0}{\varepsilon} \right| \times 100$ and similar definitions apply for the remaining error quantities.

Table 1. Maximum relative errors associated with the expessions for ε_0 , ε_1 , and ε_2; the quantity e_0' is defined as: $e_0' = \max \left| \frac{\varepsilon - \varepsilon_0}{\varepsilon'} \right| \times 100$ and similar definitions apply for the remaining error quantities.

Maximum Error, %	$\tau\sqrt{\lvert\varepsilon\rvert} / \lambda_0 = 0.01$			$\tau\sqrt{\lvert\varepsilon\rvert} / \lambda_0 = 0.05$		
	$\varepsilon'' / \varepsilon'$			$\varepsilon'' / \varepsilon'$		
	10^{-2}	10^{-1}	1	10^{-2}	10^{-1}	1
e_0'	0.114	0.341	2.920	3.107	2.672	17.05
e_0''	182.8	18.35	1.445	934.0	96.70	10.11
e_1'	0.127	0.124	0.060	3.293	3.216	1.916
e_1''	0.434	0.267	0.018	33.06	8.629	2.727
e_2'	0.063	0.062	0.029	1.538	1.506	0.866
e_2''	0.215	0.132	0.091	15.11	3.926	2.238

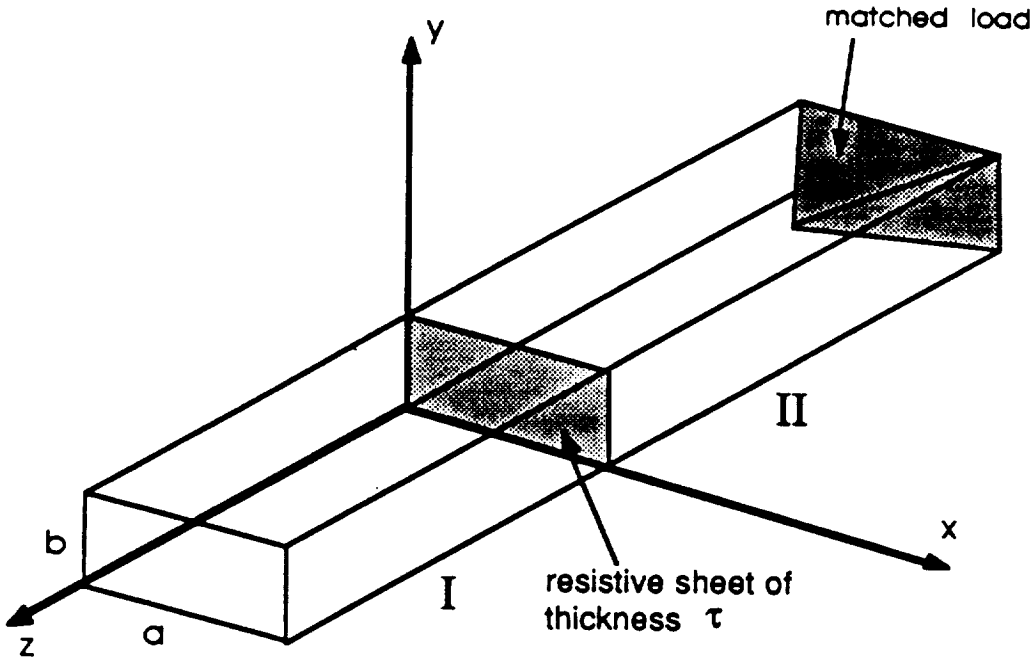

Fig. 1

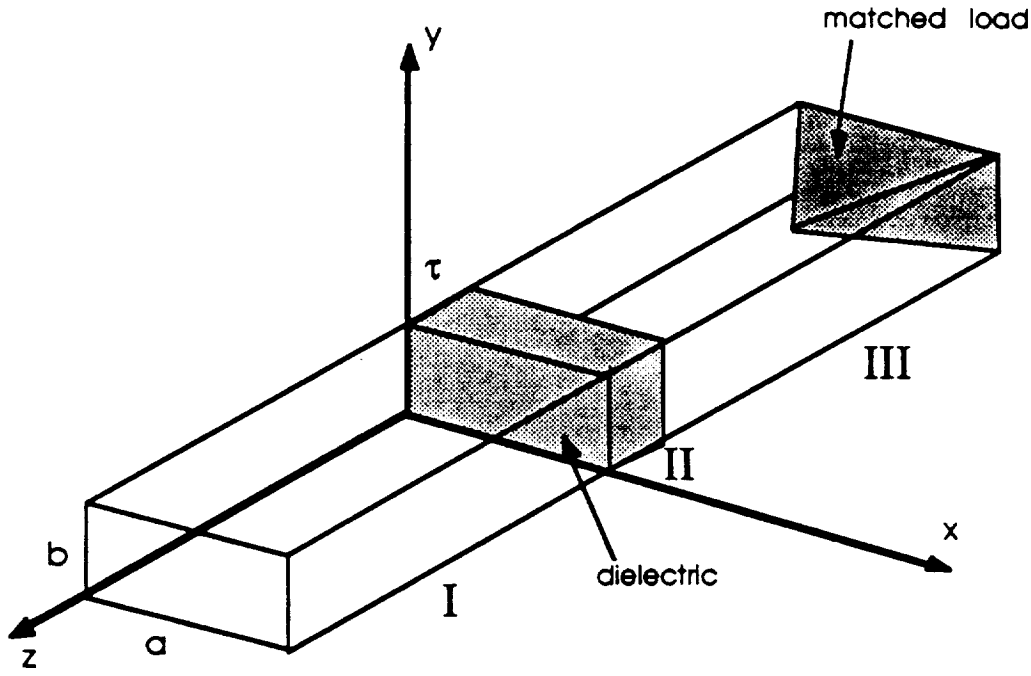

ig. 2

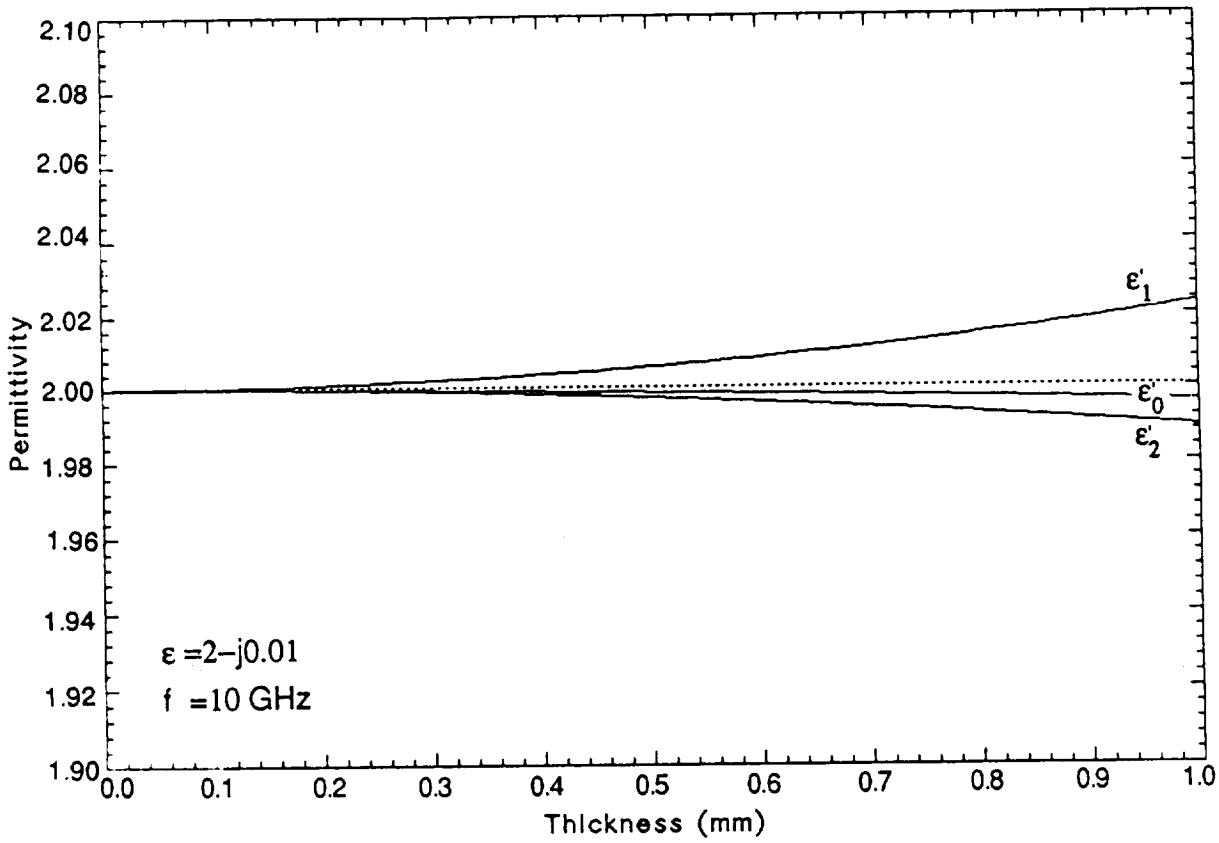

(a) Permittivity

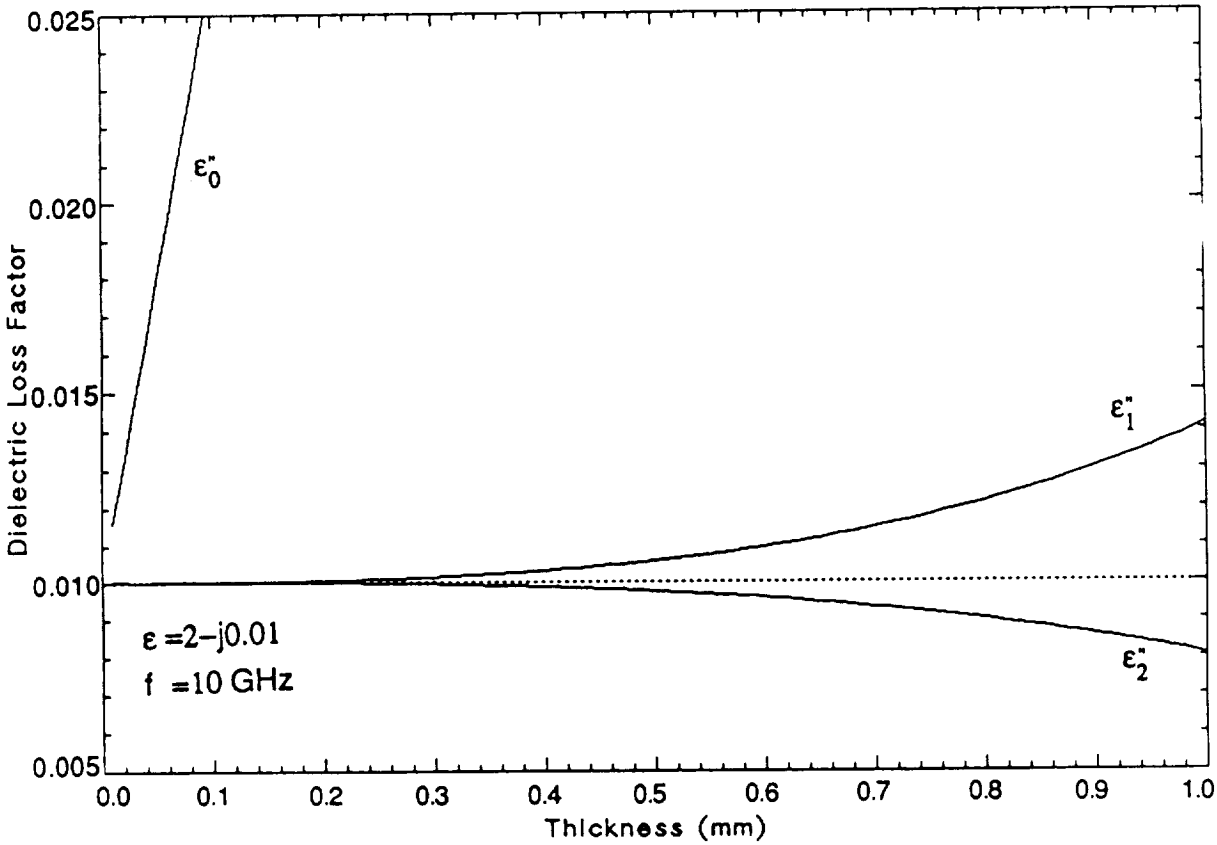

(b) Loss Factor

Fig. 3a & 3B
Sarabandi & Ulab

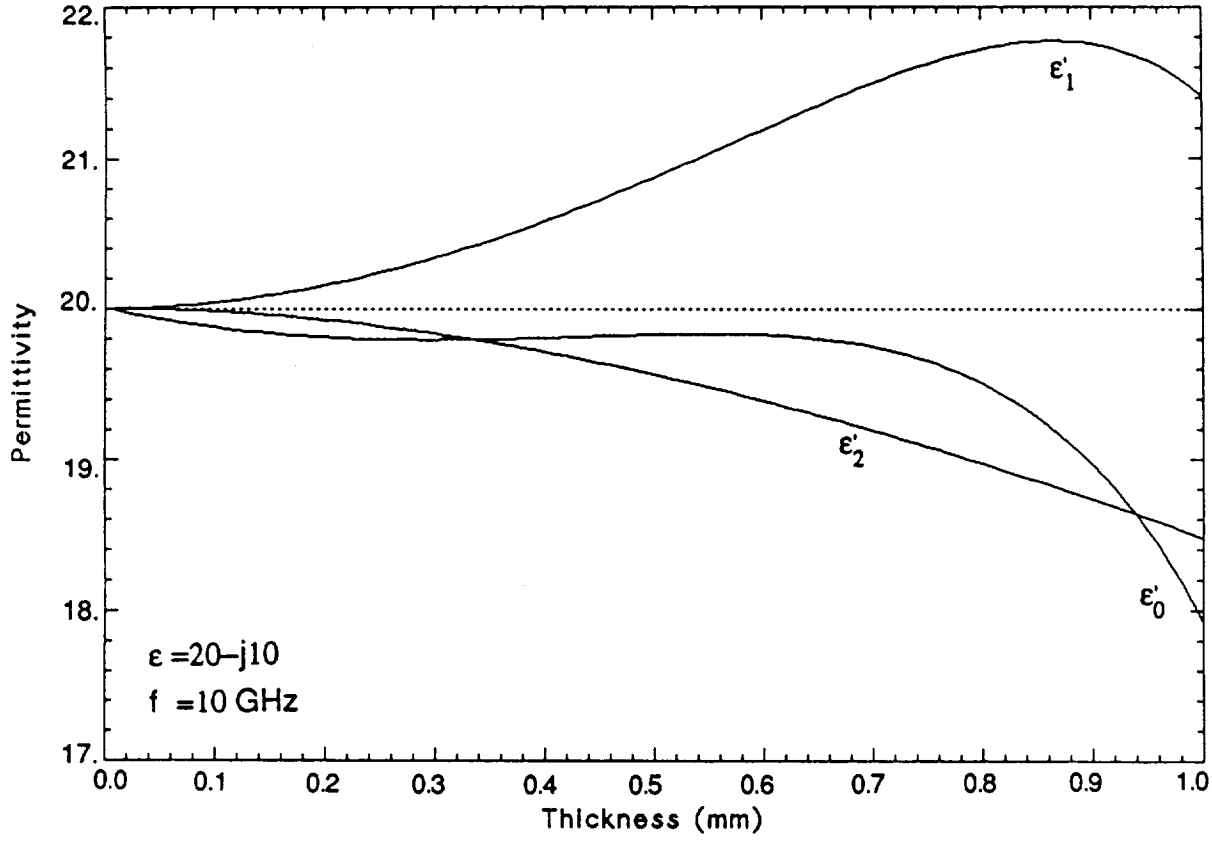

(a) Permittivity

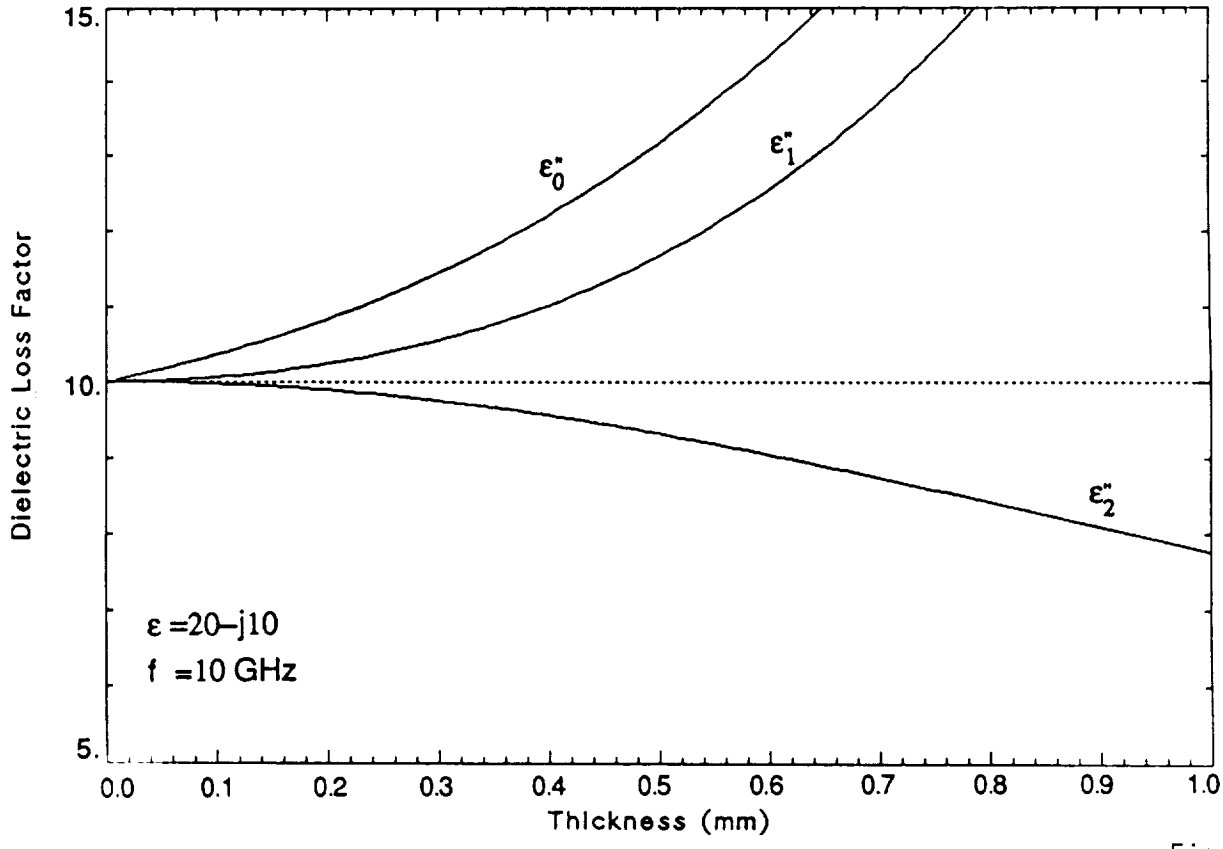

(b) Loss Factor

Fig. 4a & 4b
Sarabandi & Ula

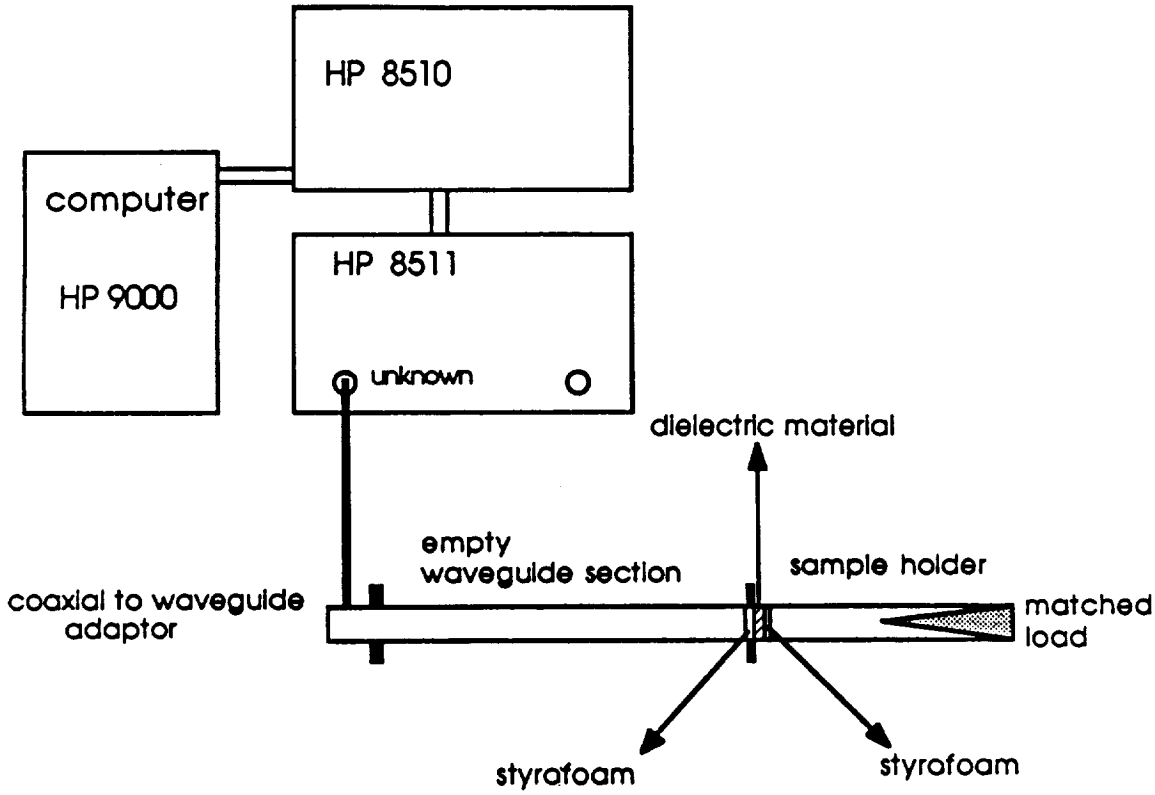

Fig. 5
Sarabandi & Ul

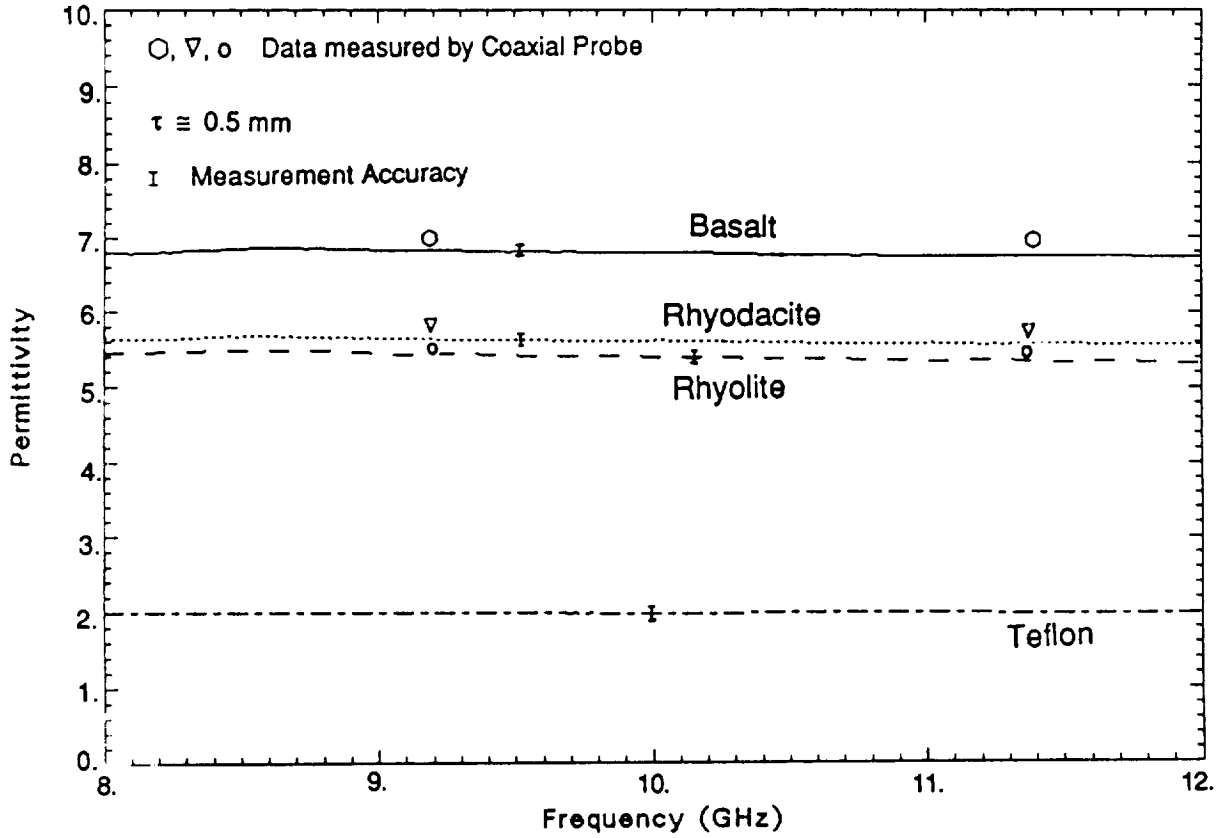

(a) Permittivity

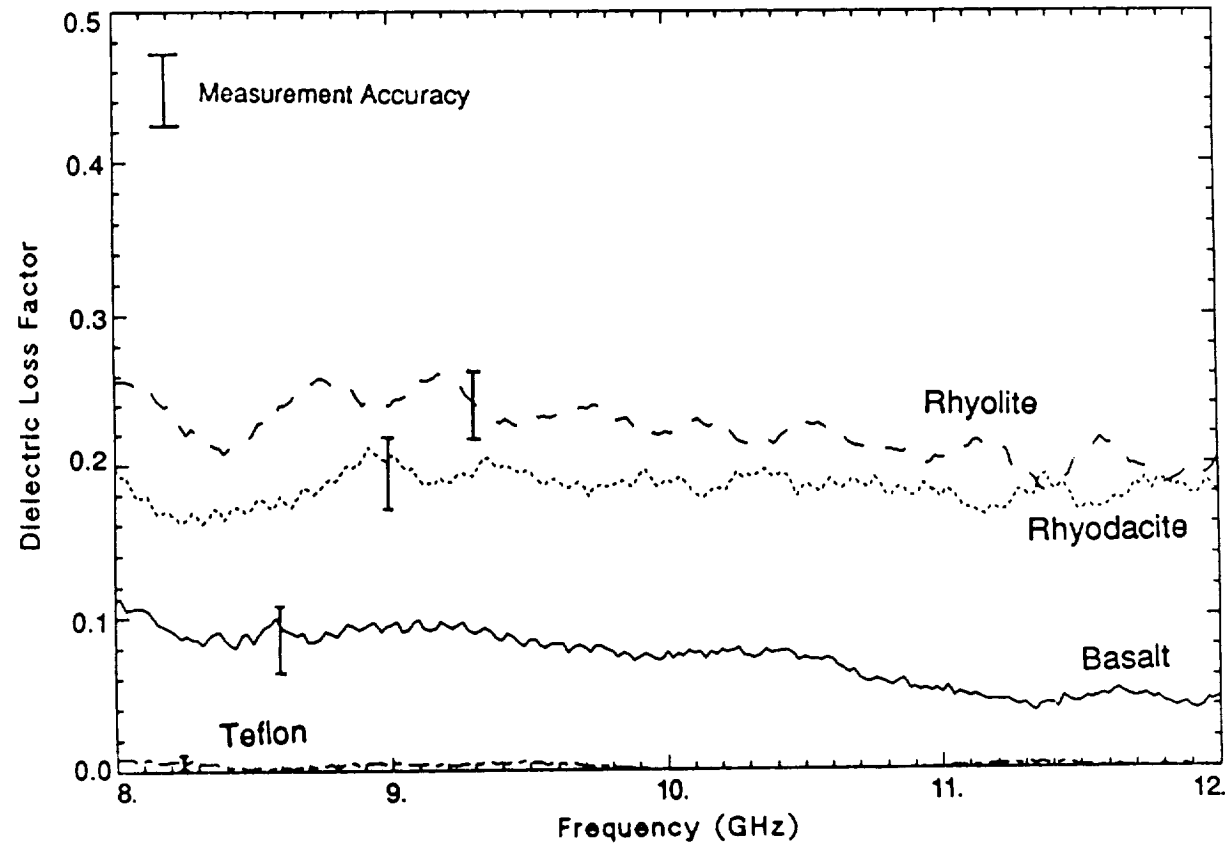

(b) Loss Factor

Fig. 6a & 6b
Sarabandi & Ula

Fig. 7
Sarabandi & [illegible]